Universiteit Utrecht

Faculty of Science - Experimental Physics

Feasibility study of the reconstruction of $D^*(2010)^+$ mesons at low transverse momentum with ALICE detector at LHC

Bachelor Thesis

Rein Perton

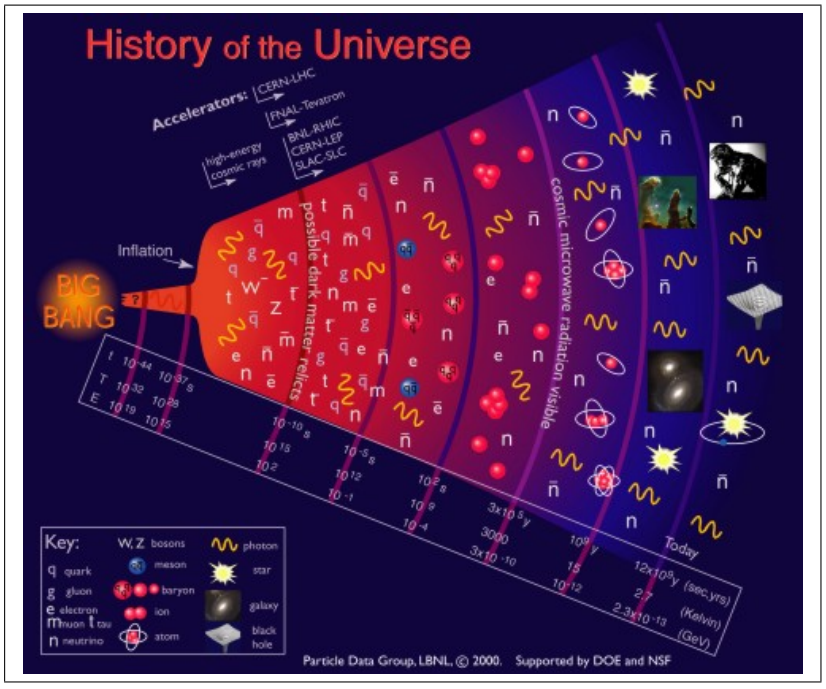

Supervisors:

Dr. A. Grelli
Utrecht University - Experimental Physics

S. Jaelani MSc
Utrecht University - Experimental Physics

06-01-2019

Abstract

Quantum Chromodynamics predicts that under condition of extreme temperature and/or pressure the ordinary matter undergoes a phase transition to the so called Quark-Gluon-Plasma (QGP) [2]. Contrary to ordinary matter, in QGP the quarks and gluons are deconfined and therefore free to move. In addition QGP is believed to have been the state of matter in our early Universe, a few microseconds after the Big Bang. In order to study its properties, QGP is reproduced in laboratory via heavy ion collisions. Due to the short lifetime ($\sim 10^{-15}$ s) and the small size ($\sim 10^{-15}$ m) of the plasma produced, the only possibility of studying its properties is by using probes. One of the most effective probes is the charm quark. The idea is to measure the modification of the production of particles containing a charm quark in a system where QGP is produced, like lead-lead (Pb-Pb) collisions at the Large Hadron Collider (LHC) [4], with respect a system where QGP is not formed, like proton-proton (p-p) collisions. Any modification can then be attributed to the charm quark energy loss in the hot and dense QCD matter, driven by key properties of the plasma like density and/or viscosity. In this thesis, we study the possibility of reconstructing the D^* particle, a charmed meson, in p-p collisions at low transverse momentum. Besides constituting the necessary baseline for Pb-Pb studies, the measurement of the production of D mesons is a key observable to test perturbative QCD calculations.

The image on the front page shows a sketch describing the evolution of the universe in terms of particle composition [1]. It shows the production of the Quark-Gluon Plasma with the proper timescales indicated.

Contents

1 Introduction

Cosmological models predict that, in our early Universe, a few microseconds after the Big Bang, all matter was in a plasma state called the Quark Gluon-Plasma [2] (QGP), with all quarks and gluons able to move in a fluid-like manner. This plasma contained quarks, the elementary building stones of hadrons, and gluons, which keep the quarks bound together in the ordinary hardonic matter, i.e. protons and neutrons. This principle is commonly known in Quantum Chromo Dynamics (QCD), as confinement. Quarks have never been observed in isolation. However, in the QGP confinement breaks down, and quarks are no longer bound by strong force into hadrons, which allows them to move as if constituents of a fluid. QCD predicts, that in order for a substance, which defies confinement, to exist, it needs to be at either extremely high temperature, density or a combination of the two, see figure 1. Conditions like these, similar to the beginning of the universe can nowadays be recreated in particle accelerators like the Large Hadron Collider [4] (LHC) at Cern in Geneva.

The LHC is currently, with a length of 27 km, the largest particle accelerator in the world. Two particle beams are accelerated within a tube, which is kept at ultrahigh vacuum, to approximately 0.999999990 c which comes down to 3.1 m/s slower than the speed of light. Superconducting magnets are used to guide the particle beams along the tube and accelerate them. Along this accelerator, detectors are placed to measure the particles which are produced during the collision of the two particle beams. LHC can accelerate and collide heavy ions, like Pb-Pb, at a maximum center of mass energy of 5.02 TeV and p-p collisions at a mass energy of 13 TeV. One of the 4 main experiments at the LHC, is ALICE [5]. ALICE is the only detector which is dedicated to the study of the hot and dense QCD matter produced in heavy-ion collisions. This detector will be discussed in section 2.

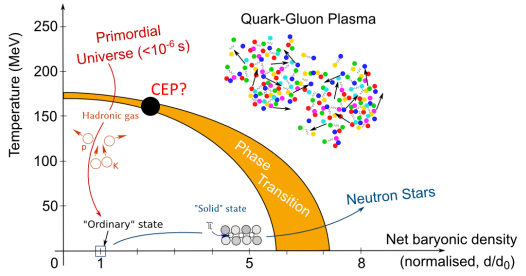

Figure 1: This figure shows the Quantum Chromo Dynamics phase diagram. The QGP is located top right in this diagram, meaning it requires high densities, high temperatures, or a combination of both to exist. [3]

The lifespan of the QGP created in Pb-Pb collisions is very short, order of magnitude of 10 fm^{-1}. This implies that doing direct measurements onto the plasma is impossible, since by the time it would reach our nearest detector ($\sim$ 3 cm) it has ceased to exist. An indirect way of measuring the plasma is therefore necessary. This is done through the use of probes. Heavy-quarks (i.e. charm and beauty) are among the most effective probes. This is because they are produced right after the collision, before the QGP, and they lose less energy traversing the plasma compared to quarks and gluons. These reasons make the heavy quarks able to penetrate the plasma better than light quarks or gluons.

While traversing the plasma, the probes lose momentum through scattering of the particles inside it. The production of a heavy-quark in heavy-ion collisions, like Pb-Pb, is compared to the production of that same quark in a p-p collision, where the hot and dense QCD matter is not formed. From this comparison, properties of the plasma can be determined based on the modification of the production rate of our probe among the two systems.

However, it is impossible to detect individual quarks using modern experiments, since they are confined into hadrons outside of the QGP. Therefore, particles that contain the quark of interest, in this thesis the charm quark, have to be found and investigated. The D^{*+} meson can be used to investigate the properties of the charm quark. By investigating transverse momentum (further referred to as p_T) dependent production probability of the D^* meson in p-p and Pb-Pb collisions, it is then possible to infer the energy loss of the charm quark and extract key plasma properties.

In this thesis the feasibility of reconstructing the D^* meson at low p_T (0-8 GeV) is investigated. This is done by simulating collisions and selecting a specific decay chain, section 3.1. Then we study kinematical variables and find topological cuts on the momentum of particles that reduce the combinatorial background, while keeping most of the signal, and we run those cuts in data to investigate if the cuts made the D^* peak in the invariant mass plot visible. The final goal of this research project is to establish the minimum possible p_T at which the D^* meson can be reconstructed and to improve the quality of the signal extraction by optimizing the kinematical selections on the daughter particles.

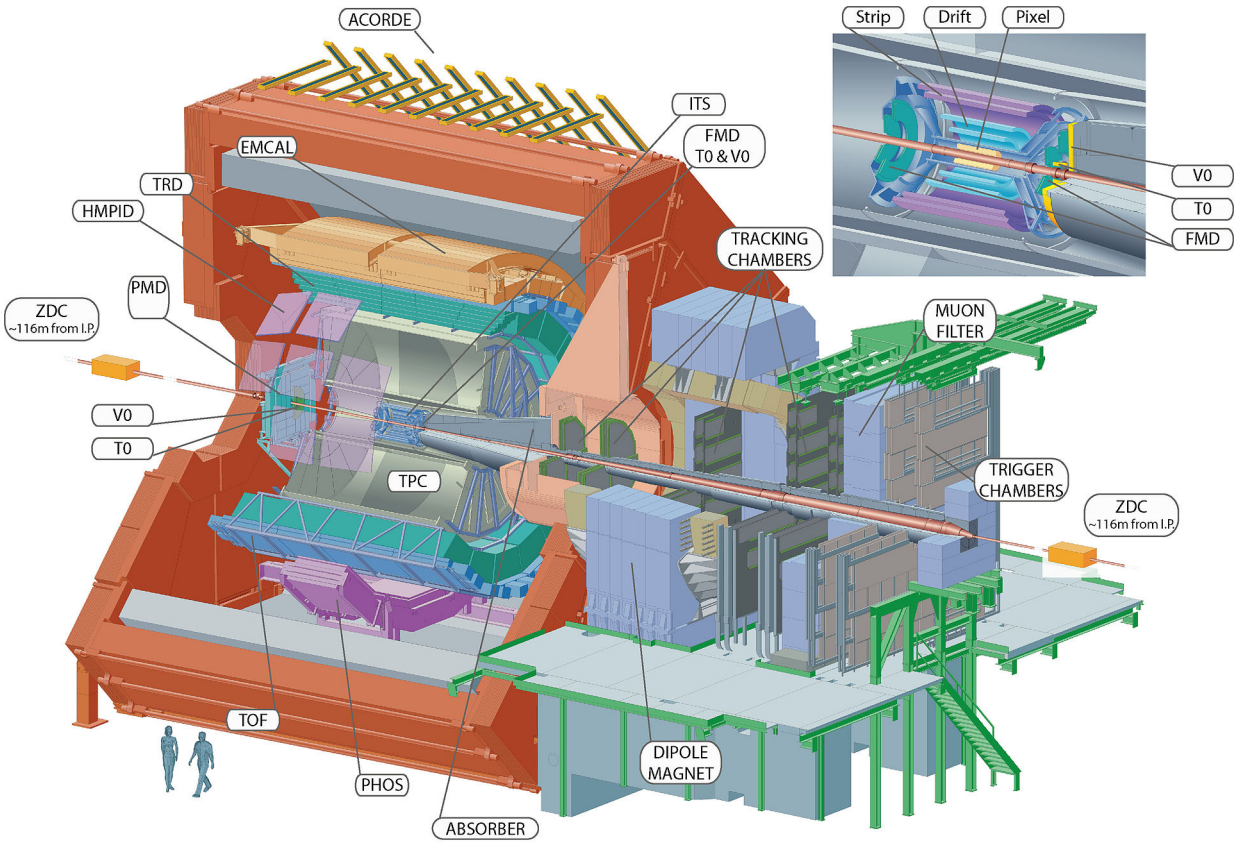

Figure 2: This picture shows a schematic view of the ALICE detector at the LHC. All detectors within ALICE are shown. The enlarged picture shows the Inner Tracking System (ITS) detector in more detail. [6]

2 ALICE detector

The ALICE detector is a heavy-ion detector, built for studying matter at extreme energy densities, where QGP forms. ALICE is 26m long, 16m high, 16m wide and weighs over 10.000 tonne. Figure 2 shows that ALICE contains over 15 individual detectors, all serving their own purpose. This thesis, however, builds mainly upon three of them, which will be discussed in the following subsections.

2.1 Inner Tracking System

The Inner Tracking System [7] (ITS) is a silicon based detector which can be found at a distance of 3.9 cm up to 43 cm from the beam. Due to it being so close to the collision event, it is possible for the detector to measure particles at very low momentum (p > 60 MeV). From the inside out it consists of 2 Silicon Pixel Detectors (SPD), followed by two layers of Silicon Drift Detectors (SDD) and ultimately two layers of Silicon Strip Detectors (SSD), see figure 3. The main focus of the ITS detector is to reconstruct primary and secondary vertices, which will be elaborated on in section 3, as well as improving the tracking of particles near the point of interaction. Moreover, the ITS measures particles that either do not have the momentum necessary to reach or are missed by the external tracking detectors, like the Time Projection Chamer or the Time of Flight detector. Since the ITS detector consists of 6 layers, it logically follow that it provides us with only 6 tracking points. However, these points are at very high resolution, and therefore give us very precise information about the tracks close to the vertices, which is extremely important for particle reconstruction, as will be discussed in section 3.

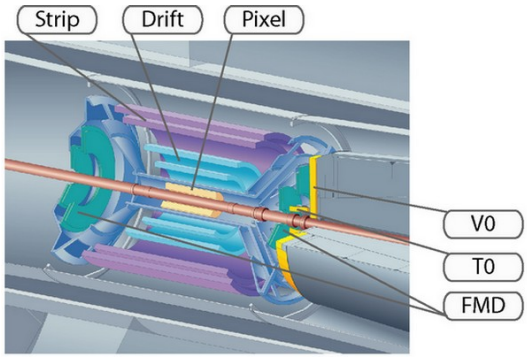

Figure 3: The ITS of the ALICE detector is shown above. You can see the division into the 3 pairs of silicon layers: SPD, SDD and SSD. [8]

The SPD is designed to provide ALICE with information about the secondary vertex of charm and beauty hadron decays. In this region there are up to 8000 particle multiplicity, which makes it incredibly hard to extract this information. The SPD can detect anything within the pseudorapidity of $|\eta| < 1.95$. These two layers are located at 39 mm and 70 mm away from the beam pipe. The two pixel detectors, also called ladders, are made out of 5 readout chips, which are arranged in a matrix of 32 columns and 256 rows of pixels. This means that the detector can detect anything that goes through roughly 21250 μm^2, as long as the trigger is above the threshold.

The SDD is found in the middle of the ITS, and consists of 0.3 mm thick silicon wafers. The idea behind this detector is that when a particle crosses the width of an SDD, electrons are released, which drift following the effects of an applied electric field. These electrons then end up at an array of 256 anodes, from which the drift time and therefore the y coordinate can be calculated. The x coordinate comes from the place of the anode where the electron was measured.

The final and most outer detector which we will discuss of the ITS, is the SSD. These two layers provide crucial information in the tracking of a particle, since it connects the information from the tracks of a particle of the external detectors (TPC), which will be discussed later on this section, with the information of the ITS. It also measures energy loss, which contributes to particle identification.

2.2 Time Projection Chamber

The Time Projection Chamber [9] (TPC) which is relatively large compared to the ITS. Being 60 cm up to 250 cm away from the beam, and following the beam tube for over 5 m, this detector has a total sensitive volume of 88 m^2. The TPC is the main detector when it comes to particle tracking in the central barrel. It can measure particles with low momentum (p > 100 MeV) and is able to provide up to 160 points along the track of a particle. However, unfortunately, these points are at a much lower resolution than the ITS detector. Furthermore, when combined with other detectors like the ITS, it can be used to study for example meson resonances, but also charm and beauty quarks. The TPC is also used for particle identification through energy loss, since for most particles, this is unique, see figure 4.

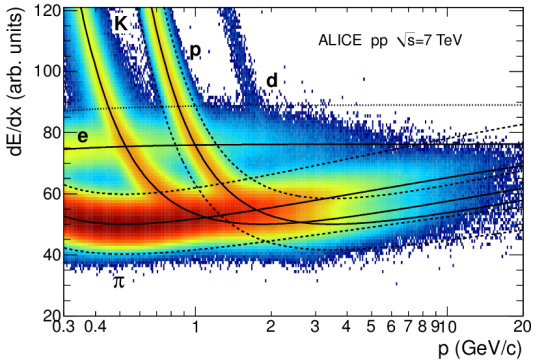

Figure 4: Above, an image of the specific energy loss detected in the TPC of ALICE is shown. [10]

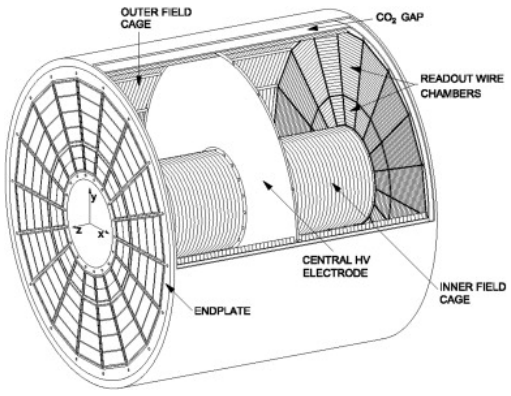

Figure 5: This figure shows the basic layout of the TPC in the ALICE detector at the LHC. [11]

Essentially the TPC is a cylinder filled with 90% Ne - 10% CO_2 gas, and is divided into two drift regions through a central electrode. This gas is used because it is found to be the optimum considering charge transport, signal amplification and transparency for traversing particles. An external uniform electric field along the symmetry axis of the TPC is applied through the outer- and innerfield cages to the chamber, making charged particles traverse the volume of the detector, ionizing the gas. These free electrons then drift towards the edges of the detector. Where the signal is extracted from, after it has been amplified using an avalanche effect near the anode wires, by the readout wire chambers.

2.3 Time Of Flight

The Time Of Flight detector [12] (TOF) is primarily made to provide particle identification of charged particles over a very large part of the phase space. It has a cylindrical shape and covers all polar angles between 45 and 135 degrees all the way around the collision. The cylinder is divided in the azimuth into 18 parts, each of them didived into 5 so called modules, which in turn contain 1593 detector elements (Multigap Resistive Plain Chamber strips). In total this detector with an inner radius of 3.7 m and close to 160.000 MRPCs, spans an area of 141 m^2.

A MRPC is a stack of resistive plates made out of glass, with an anode pickup electrode in the middle and cathode pickup electrodes on the outside, see figure 6. A high voltage is put onto the external surfaces of this stack of glass plates. Which induces a strong electric field. When a charged particle ionizes the gas, this ionization is amplified by the electric field creating an avalanche effect. However, this avalanche is stopped from preceding across the entire MRPC by the resistive glass plates, which are made in such a way that they are permeable to the signal induced by the electrons on the pickup electrodes. This signal is therefore the total of all gaps in between the glass plates. The more gaps, the higher efficiency is achieved, however, the time resolution is based upon the with of the gaps in between the planes, the narrower the gap, the better the time resolution will be.

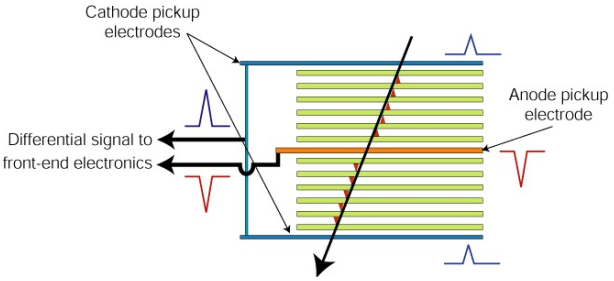

Figure 6: This figure shows the underlaying structure of a MRPC element from the TOF detector in ALICE at LHC. The resistive glass is shown in green.[12]

3 Theory and Methodology

Exploring the properties of the QGP can be challenging, since the lifespan of the plasma that can be created is of order 10 fm^{-1} ($\sim 10^{-15}$ s). This is because it expands very rapidly, which causes temperature and pressure to drop. Since this hot and dense matter can only exist at these extreme conditions, it is impossible to measure directly, as it does not reach the detectors before it ceases to exist. This means the QGP can only be measured indirectly, using a probe. Through this probe, which traverses through the plasma, it is possible to extract certain properties, e.g. angular momentum, density, temperature, viscosity, etc. etc.. This is done by allowing it to interact (or collide) with the particles inside the medium. The interaction of the probe with the plasma, leaves an imprint that can be used to deduct the QGP properties. Therefore, the longer a probe traverses through the plasma, the more information it will gather. However, it is obvious that the probe has to emerge from the QCD matter, in order to allow us to extract the information.

3.1 Determining the probe

Since the Quark-Gluon Plasma has a lifespan of order 10^{-15} s it cannot be measured by any existing instrument. Therefore, a probe needs to be found that is possibly created before the production of the plasma, traverses it while interacting and finally emerges carrying the information gathered from the QGP. It is known that the production time of quarks is inversely proportional to their mass,

$$\Delta t \propto \frac{1}{m}. \tag{1}$$

Once we apply formula 1 to the known quarks there are only a few that can be considered good probes. Among them the most promising are the heavy quarks: charm, beauty and top. However, there is a problem with the latter two. Both the beauty as well as the top quarks due to their respective masses [13] of 4.19 GeV/c^2 and 172 GeV/c^2 are extremely rare, since it requires large energy to produce them. This means that both the beauty as well as top quarks are formed way less then the charm quark. Therefore, in order to get good statistics, the charm quark is the most promising probe that can be used. The charm formation time is approximately 0.06 fm^{-1} and therefore is produced before the QGP, which has a formation time of around 1 fm^{-1}. In addition the charm quark is relatively heavy and is, therefore, expected to lose less energy while interacting with the hot dense QCD matter, traversing it entirely and emerging, so that it can hadronise into particles whose decay products can be detected, than light quarks and gluons (due to the so called dead cone effect [14] and color charge effect [15]). Finally, due to its large mass (1.27 GeV/c^2) [13] it is unlikely for the charm quark to be thermally produced in the plasma itself. This makes it a clean penetrating probe. Unfortunately, the charm quark does not remain stable by itself, since quarks are confined into hadrons to form the ordinary matter. This means that it ultimately hadronises into particles. In this thesis, we consider:

$$c + \bar{d} \rightarrow D^*(2010)^+, \tag{2}$$

$$D^*(2010)^+ \rightarrow D^0 + \pi^+, \tag{3}$$

$$D^0 + \pi^+ \rightarrow K^+ + \pi^- + \pi^+. \tag{4}$$

Formula 2 describes the charm quark which produces a $D^*(2010)^+$ when it pairs with an anti-down quark. However, this $D^*(2010)^+$ is unstable and decays as well. Formula 3 shows the $D^*(2010)^+$ mode chosen for the analysis with a branching ratio (BR) of 67.7%. There are many more, but this is the most common one. It is not yet finished, since the D^0 particle is not a final particle either. This particle also decays after approximately 100 μm, and in formula 4 the specific decay chain chosen for the analysis ($BR \sim 3.9\%$) is shown.

3.2 Finding the probe

The ITS, TPC and TOF detectors, mentioned in section 2, are able to track and identify particles. However, since the D^* as well as the D^0 are unstable particles that decay within at most $\sim$ 100 μm from the creation point in the ALICE detector, only the final state (long living) particles, the kaon and the pions, can be tracked. Therefore, to understand if the kaons and pions that are tracked belong to the decay of interest, an invariant mass analysis is performed with the aim to reconstruct the D mesons and extract the signal. This procedure starts with trying to pair each kaon and pion in the detector. This is how the so called "D^0 candidate" is made. The vast majority of these candidates will not be true D^0 mesons but will instead be combinatorial background (i.e. the pion and kaons used to form the candidate are random tracks, not arising from a true D^0 decay).

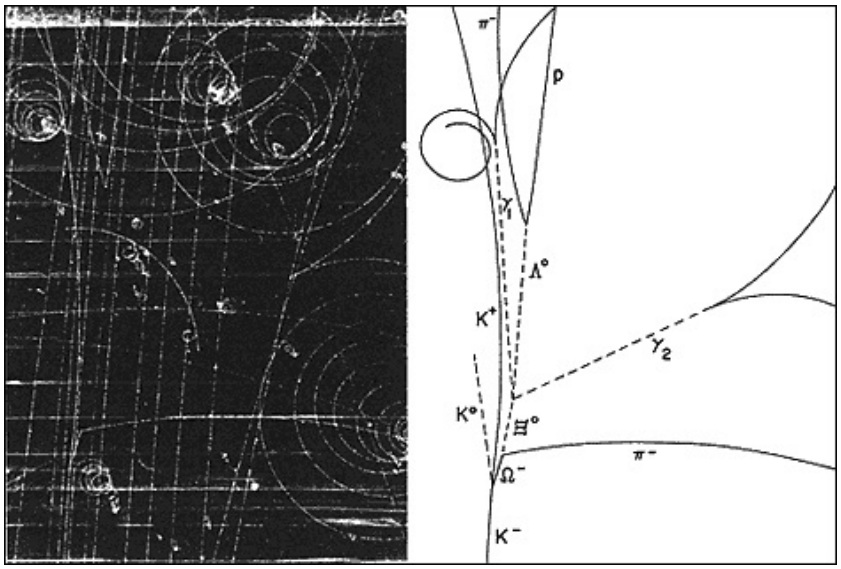

Figure 7: This image shows the principle of particle reconstruction, specifically it shows the discovery of the ω^- particle. Note, this is not a representation of the D^0 candidate, it is merely meant to illustrate the method. [16]

The following step entails selections based on some criteria. For example, the two tracks that make the candidate have to come from a common secondary vertex, where the D^0 decay took place, see figure 7. This implies a criteria based on the two tracks having a distance of closest approach to each other which defines if they come from the same secondary vertex. This distance is set to approximately 200 μm. After these selections are made, the combinatorial background is reduced by several orders of magnitude. Additional help in reducing this background is given by particle identification. After all selections are applied, the true D^0 particles show as a gaussian peak on the invariant mass ($M(K\pi)$) plot.

The final step in reconstructing the D^* meson consists of adding a pion track to the D^0 candidate and calculate the invariant mass ($M(K\pi\pi)$) of the particle triplet. The D^* meson signal will then appear as a gaussian centered at around 145.42 MeV/c^2 in the mass difference between the $M(K\pi\pi)$ and the $M(K\pi)$ invariant masses.

3.3 Topological cuts

In sections 3.1 and 3.2 the need to apply selections when reconstructing the D^* meson in order to suppress the combinatorial background was discussed. These selections are called "topological cuts" as they are based on the topology of the decay of interest. Currently, 16 topological cuts are made in order to reconstruct the position and momentum of the D^*. These cuts are made to reduce the background while trying to keep as much signal as possible, for statistical purposes. It is impossible to cut away background without cutting away part of the signal as well, so compromises have to be made. In this thesis cuts based on the momentum of the pion coming from the D^* decay mentioned in formula 3 (referred to as soft pions) are researched and applied.

One of the main topological cuts is very shortly mentioned earlier in subsection 3.2, namely the Distance of Closest Approach (DCA). The DCA determines the maximum distance two of the daughter particles can be separated from each other at the point of closest approach for them to be considered to come from the same mother particle. In ALICE, this DCA is set to approximately 150 μm - 300 μm. So when an attempt is made to pair a pion and kaon in order to find the D^0 candidate, the pion and kaon tracks have to get within 150 μm (for high transverse momentum candidates) to 300 μm (for low momentum candidates) of each other in order to be accepted as a legitimate candidate.

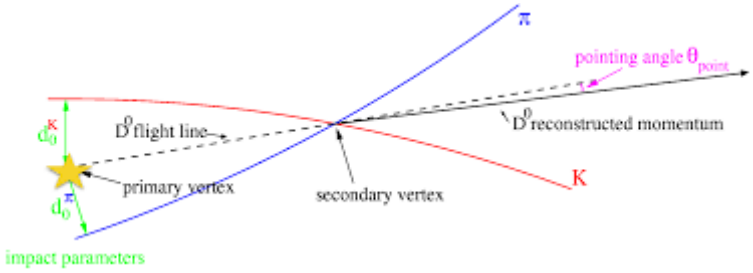

Figure 8: This figure illustrates the pointing angle of a particle. [17]

A second important topological cut it the so called "cosine of pointing angle". The pointing angle is defined as the angle between the flight line of the mother particle, and the reconstructed momentum. The momentum is reconstructed by applying conservation of momentum on the kaon and pion. In figure 8, the pointing angle is illustrated for the D^0 decay. Taking the cosine of this angle implies a value of 1 means the flight line and reconstructed momentum are aligned. Clearly genuine D^0 mesons will tend to have the reconstructed momentum aligned with the flight line, while combinatorial background will have a much weaker correlation between the reconstructed candidate momentum and the flight line.

4 Data Analysis

The idea of this thesis project was to find cuts based on the p_t values of the soft pions for different intervals of p_t of the mother particle, the D^*, assess them and evaluate the result, to see if extracting signal at low p_t of the D^* would be possible. In order to find cuts, a simulation had to be run in which the particles and their properties needed for the cut were stored. This meant a collision of two protons had to be simulated, then a selection had to be applied on all particles, to only get the particles following the decay sequence as mentioned in section 3.1 formulas 2, 3 and 4. Once that was done, the necessary properties of those particles had to be stored to be able to compare them to the data. This whole procedure was done with the help of mainly two software programs: PYTHIA8 [18] and ROOT6 [19].

4.1 PYTHIA 8

PYTHIA is a program which is designed to generate high-energy physics event, like the collision of particles at high energies. The program contains theory and models for a lot of physics aspects, to give a good representation of the event. For example, it contains information about hard and soft interactions, multiparton interactions, fragmentation and decay, parton distributions and many more. PYTHIA is based on the latest knowledge of Quantum Chromo Dynamics, complemented with the latest experimental measurements for parameter tuning.

JETSET, which was the predecessor of PYTHIA, was developed by the Lund theory group starting from 1978. Many people have contributed to making JETSET and programs based on it, of which PYTHIA was the largest. They became quite similar and therefore fused in 1997. It was written in programming language Fortran 77, until it was rewritten in 2004 to C++. This then eventually became the main version of PYTHIA.

4.2 ROOT 6

The second C++ based program that was used was called ROOT. It was developed at CERN to be a framework for data processing, and is the main program used by high-energy physicists to analyze their data or perform simulations. Especially since it can work together with other software like PYTHIA. ROOT has a lot of possibilities, mostly focussed around particle physics and data analysis. The support of the program is very large, which makes it an easy to use program.

4.3 Method

We used PYTHIA to generate events of proton-proton collisions at 13 TeV. During this event generation, a specific command was used in order to "stimulate" or "force" the production of heavy flavour quarks; "$pythia8 \rightarrow ReadString("HardQCD : all = on");$". This forcing of heavy quarks does not touch the underlying physics, it is applied solely for the reason of having to run less events to get a lot more statistical information, since it ensured at least 1 heavy quark pair was created each event. The command to generate the events would give an array full of particle information, transverse momentum, charge, daughter particles, pseudorapidity and many more as output. Based on this output, a selection could be made using ROOT commands.

First of all, only the particles that would be visible in the ALICE detector needed to be selected, in order to properly compare the simulation output with real data. This implies a limit has to be set on the pseudorapidity of each particle, in our case: $\mid \eta \mid < 0.9$. Since it is a simulation, it is known of each particle where is comes from and what other particle decayed into that particle. This information is used in order to select only those particles that are following the decay sequence as mentioned in section 3.1.

Now, in principle all particles needed were gathered, and the first results can already be shown by extracting specific information out of these particles, like the transverse momentum, see section 5 figure 9. However, ultimately this research was about investigating the transverse momentum of soft pions depending on the transverse momentum of their mother particle, the D^*, in low p_t regions of the D^*, and check if such distributions would significantly differ from the one including all background pions. If this would be the case, selections could be applied to reduce the combinatorial background. Therefore, both the soft pions as well as the pions coming from the decay of the D^0 (see formula 4 section 3.1), are divided into so called "p_t-bins". Since this thesis researched the lower p_t region of the D^* mother particle, the following bins were chosen, values are in GeV/c: [0-0.5], [0.5-1], [1-1.5], [1.5,2], [2,2.5], [2.5,3], [3,4], [4,5], [5,6], [6,7], [7,8]. The p_t-distributions are then plotted for each D^{*+} p_T-bin.

A ratio between the chance distributions of the soft pions and the chance distributions of the inclusive pions was made. This would show how likely it would be to find soft pions in a certain p_t-range at a specific p_t, compared to how likely it would be to find any pions in that range at that p_t at all. For example, if the chance distribution of the soft pion peaks at a p_t at which the chance distribution of the inclusive pions is very low in value, chances are relatively high that any pions at that p_t are soft pions. Based on this information, the cuts on the p_t values were determined. The same thing was done for the D^0 pions.

At this point in time, the cuts, determined from the ratio plots, were applied to the "real" data coming from CERN. The data used was a selection of 17 million events from the LHC15o-PbPb2015 data set. After the run finished, in particular the p_t distribution data of the soft pions found in real data was acquired in ROOT and compared to the simulation data, see section 5 figure 15. The invariant mass plots of the D^* particle were also retrieved and plotted, which can be seen in figure 16, also in section 5. The D^* invariant mass was fitted with a function describing the combinatorial background $(a * \sqrt{(x - m_\pi)} * e^{b(x-m_\pi)})$ and a Gaussian, describing the signal. For each mass plot, the statistical significance of the signal $(S/\sqrt{S+B})$ was calculated. In this formula, S is the yield of the gaussian signal over a region $+/-3\sigma$ and B is the total yield of the background in the same region.

5 Results

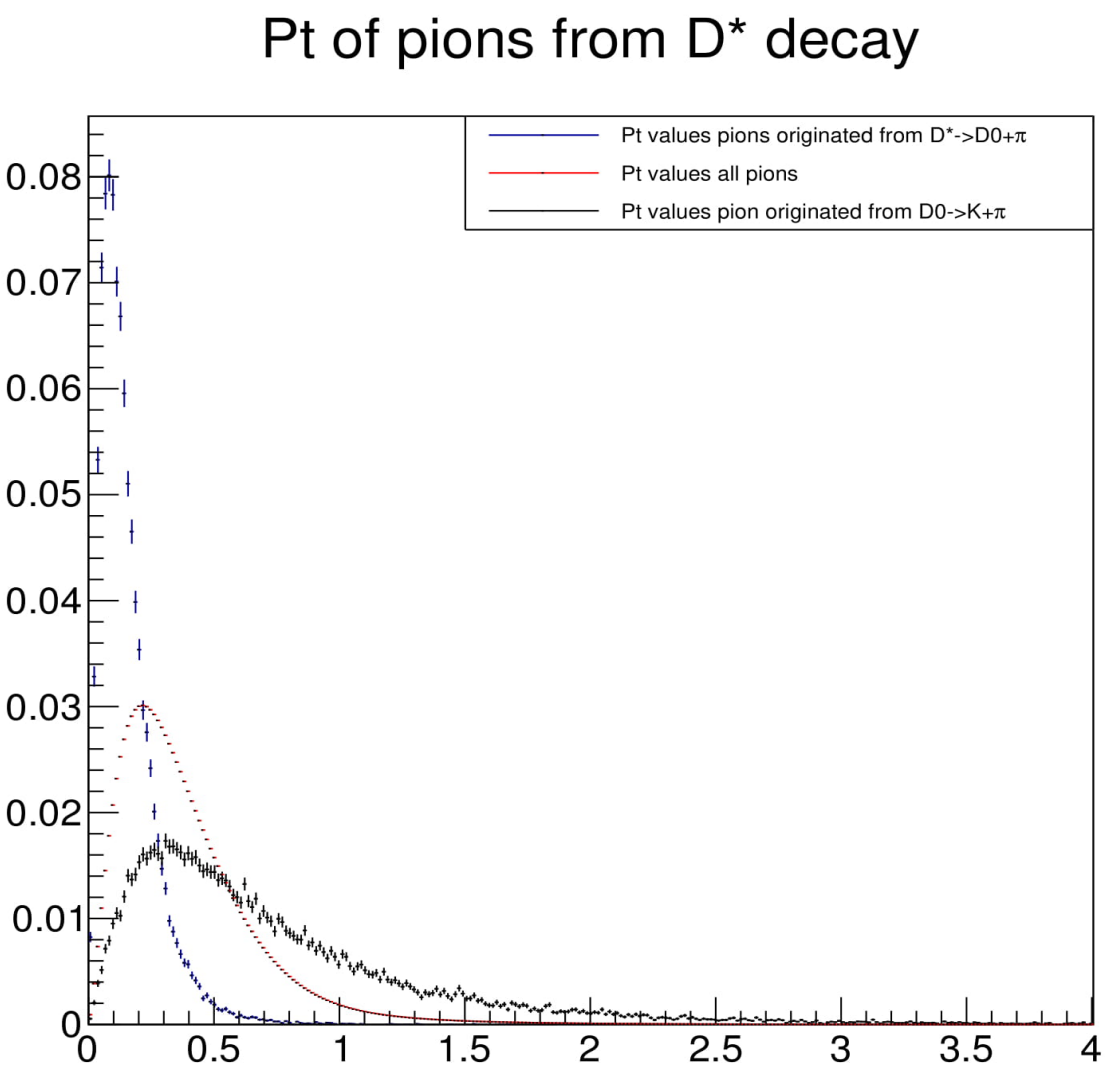

Figure 9: This figure shows the p_T distributions of the soft pions (in blue), the D^0 pions (in black) and the inclusive pions. The plots are evaluated D^* p_T integrated.

In figure 9 the p_t distribution of the soft pions is shown by the blue line. This distribution has a maximum at a p_t of 0.0825 GeV/c. The signal is localized around the area 0-0.5 GeV/c. Out of the 35391 soft pions that were analyzed, 624 have a p_T larger than 0.5 GeV/c, this is 1.8% of the total signal.

The red graph shows the p_t distribution of the inclusive pions produced in the collision. The peak of this distribution lies at 0.2175 GeV/c. It a relatively broad peak, compared to the soft pions, with only 3.7% of the inclusive pions having a p_T above 1 GeV/c. There are still $2.83 * 10^7$ pions which have p_T values higher than 1 GeV/c However, this amount is not significant compared to the total amount of $7.62 * 10^8$ inclusive pions.

In black, the p_t distribution of pions produced by the $D^0 \to K^+ + \pi^-$ decay is shown. This is a very broad signal with respect the p_T distribution of the soft pion. The peak of this distribution lies at 0.3075 GeV/c. The signal dies out at around 2 GeV/c, with only 1829 pions (5.1%) having a p_T larger than 2. The tail of the graph is a lot longer suggesting that D^0 pions have a relatively high transverse momentum compared to the inclusive pions.

Figure 10 shows that the correlation between the p_T of the soft pion and the D^* is much more apparent then the D^0 pion and the D^*. The lower the momentum, the stronger the correlation seems to be. This means that if the low p_{T,D^*} range is divided into narrow p_T-bins, the soft pion p_T distributions within the narrow D^* p_T-bin will be very localized, as can be seen in figure 11, allowing the isolation of these particles. However, finding these pions becomes harder, due to an increase in background through other particles having very low momentum. The correlation between the D^0 pion becomes stronger if the p_T value of the D^* particle is very low, however, the correlation between the soft pion and the D^* remains more prominent.

D^* p_T interval (GeV/c)	Peak value (GeV/c)
0-0.5	0.0375
0.5-1	0.0675
1-1.5	0.0975
1.5-2	0.0975
2-2.5	0.1725
2.5-3	0.2325
3-4	0.2325
4-5	0.2325
5-6	0.3675
6-7	0.3675
7-8	0.4125

Table 1: This table provides information on the peaks of the soft pion distributions shown in figure 11.

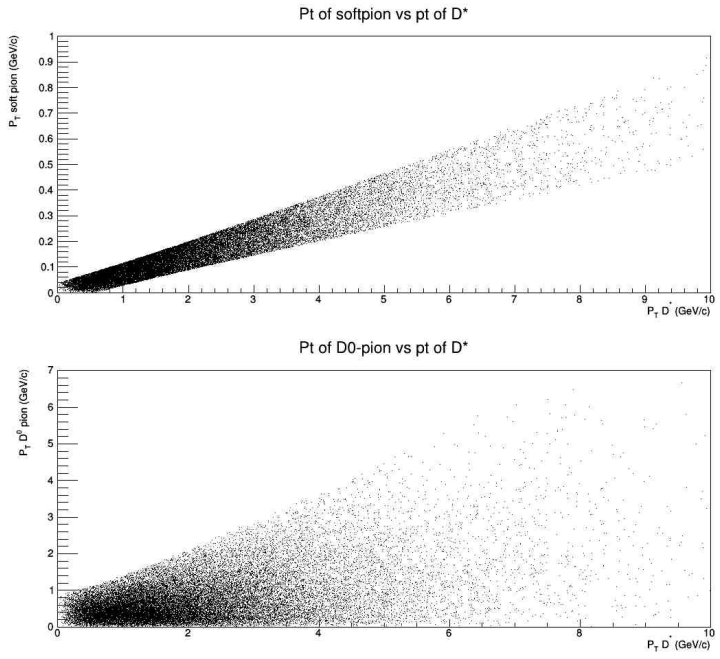

Figure 10: The top figure shows the correlation between the p_T of the soft pion and the p_T of the D^*. The bottom figure shows the correlation between the p_T of the D^0 pion and the D^* p_T

In figure 11 the p_t distributions of the soft pions coming from the D^* decay (formula 3 section 3.1) is shown in blue. The figure is divided into 11 p_T-bins based on the p_T of the D^* ranging from 0-8 GeV/c. The red graph represents the p_t-distribution of the inclusive pions produced at the collision. The figure shows that compared to the the p_t distribution of the inclusive pions, the soft pion distribution is more localized. The peak values of the distributions can be seen in table 1. At low D^* p_T the soft pions show relatively low p_T values, implying isolation of these soft pions can be done.

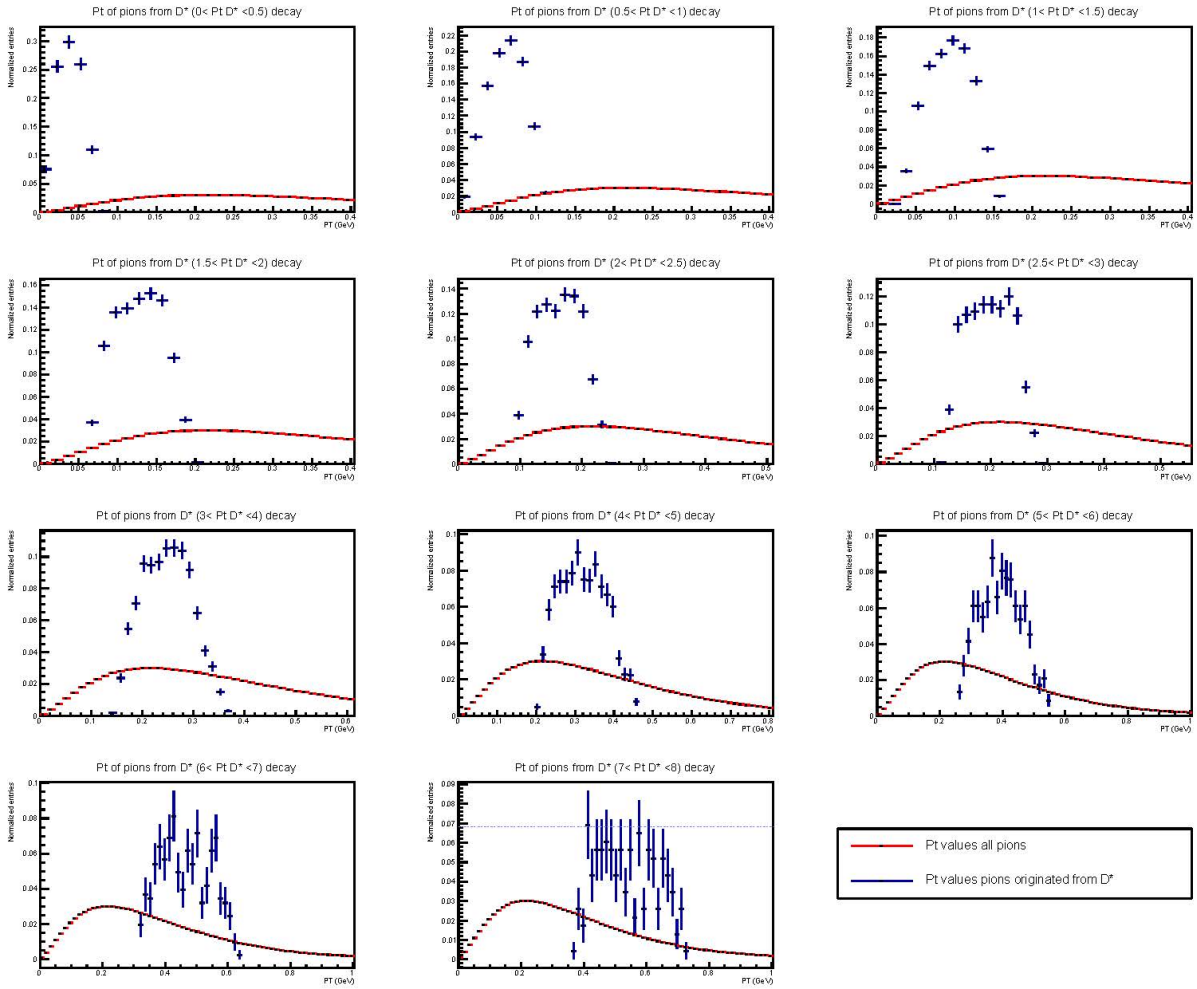

Figure 11: The p_T distributions of the soft pion (in blue), divided into the 11 investigated D^* p_T-bins ranging from 0-8 GeV/c, can be seen in this figure. The plots are superimposed by the p_T distributions of the inclusive pions.

Figure 12 shows 11 p_T distributions of the D^0 pions superimposed by the inclusive pion distribution, which corresponds to the 11 D^{*+} p_t-bins considered (section 4). The blue plots represent the p_t-distribution of the pions coming from the decay of the D^0 (formula 4 section 3.1) within the specified p_t-bins. The main peak is mostly consistent with the peak of the red graph, however, the localized distribution grows wider at higher D^* p_T values. In the higher p_t-bins, there is no longer really a clear distribution that can be distinguished, all values seem equally likely.

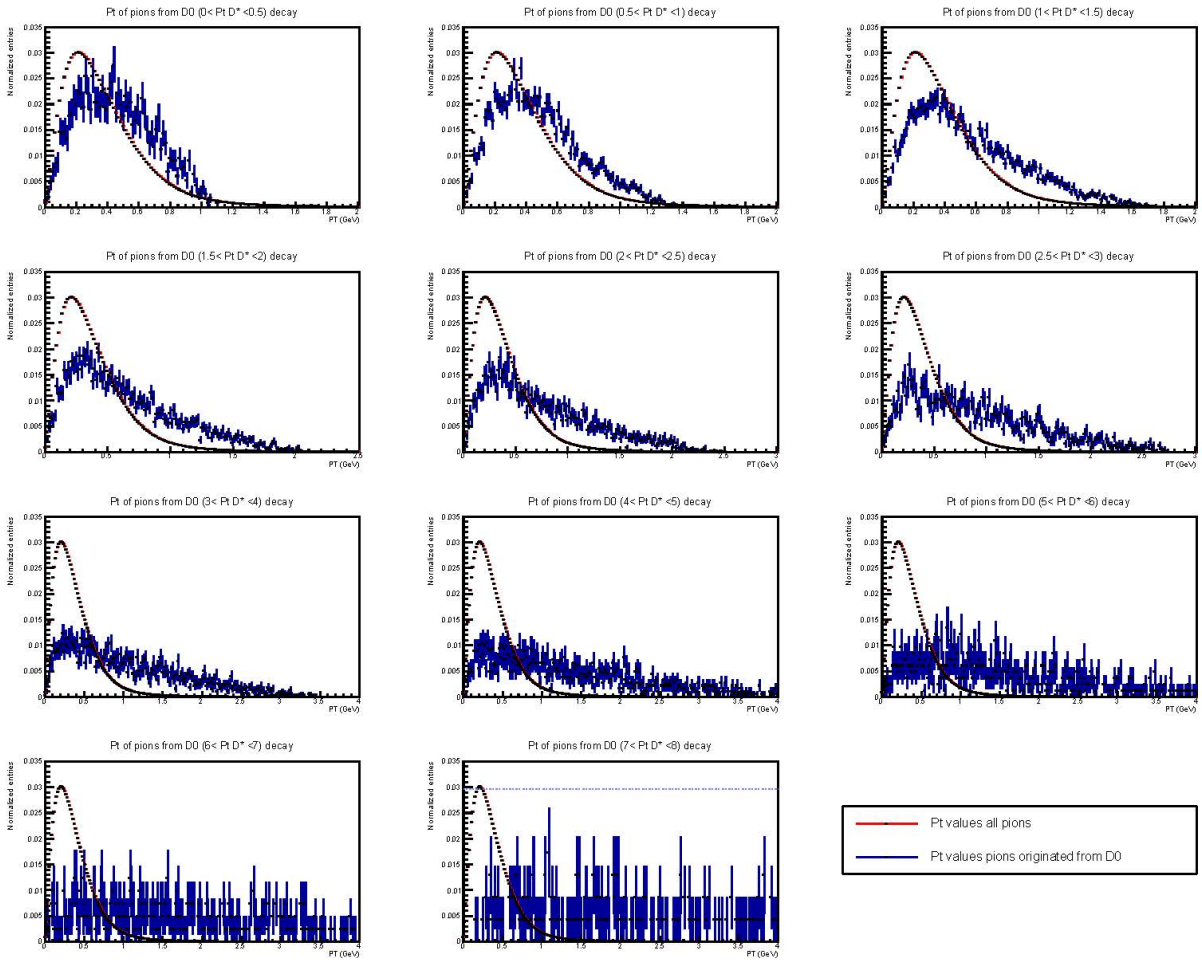

Figure 12: The p_T distributions of the soft pion, divided into the 11 investigated p_T-bins, can be seen in this figure.

Figure 10 showed that the correlation of the soft pions p_T and the D^* p_T was stronger with respect to the D^0 pions. It also showed that both correlations were stronger at lower D^* p_T values. Figure 11 shows the p_T distribution of the soft pion is localized at low D^* p_T values, and can be isolated, due to the fact that there is not much overlap between the distributions. On the contrary, figure 12 shows that the D^0 pion at low momentum is very difficult to seperate from the inclusive pions, since the overlap between both p_T distributions is quite existential. To investigate low p_T values of the D^* meson, it is therefore better to investigate the soft pion, as its momentum distribution differs more from the one of inclusive pions and therefore is more likely to offer a chance to set effective cuts to reject background.

However, the ITS detector measures particles that have a minimum p_T of 60 MeV/c and if we demand our particles have to be tracked by the TPC detector as well, in order to get sufficient tracking data, this limits the minimum p_T to 100 MeV/c. Table 2 shows the percentages of signal that can be detected based on the demands of the tracking points. It shows us that the p_T region 0-1 GeV/c does not provide us with sufficient statistical data to be able to reconstruct the D^* meson due to the intrinsic detector limitations. This means that at most, we can start reconstructing the D^* meson starting from a D^* p_T of 1 GeV/c.

D^* p_T interval (GeV/c)	% signal above 60 MeV	% signal above 100 MeV
0-0.5	10.86	0.06
0.5-1	53.71	4.85
1-1.5	85.93	42.99
1.5-2	100.00	76.17
2-2.5	100.00	98.28
2.5-3	100.00	100.00
3-4	100.00	100.00
4-5	100.00	100.00
5-6	100.00	100.00
6-7	100.00	100.00
7-8	100.00	100.00

Table 2: This table shows the percentage of pions that can be detected by the ITS ($p_T > 60$ Mev/c) and the percentage of pions that can be detected by the TPC ($p_T > 100$ MeV/c).

Figure 13, is a comparison of the two graphs displayed in each picture in figure 11. It shows the ratio of the p_t-distribution of the soft pion compare to the p_t-distribution of all of the pions. A thing to note here is that this ratio is between the normalized distributions, and does not tell us anything about the absolute values.

The cuts that were chosen for each p_t-bin were based on both figures 11 and 13, since it shows us in what p_t-rangs the soft pions are most likely to be found as well as how often they are found compared to how often pions in general are found at specific p_t-ranges. Table 3 shows the cuts per interval of D^* momentum.

D^* p_t interval (GeV/c)	Minimum cut (GeV/c)	Maximum cut (GeV/c)
0-0.5	0.02	0.06
0.5-1	0.05	0.09
1-1.5	0.05	0.13
1.5-2	0.10	0.16
2-2.5	0.13	0.19
2.5-3	0.15	0.25
3-4	0.20	0.28
4-5	0.25	0.38
5-6	0.35	0.45
6-7	0.40	0.55
7-8	0.45	0.60

Table 3: Minimum and maximum cut values per interval of D^* p_t.

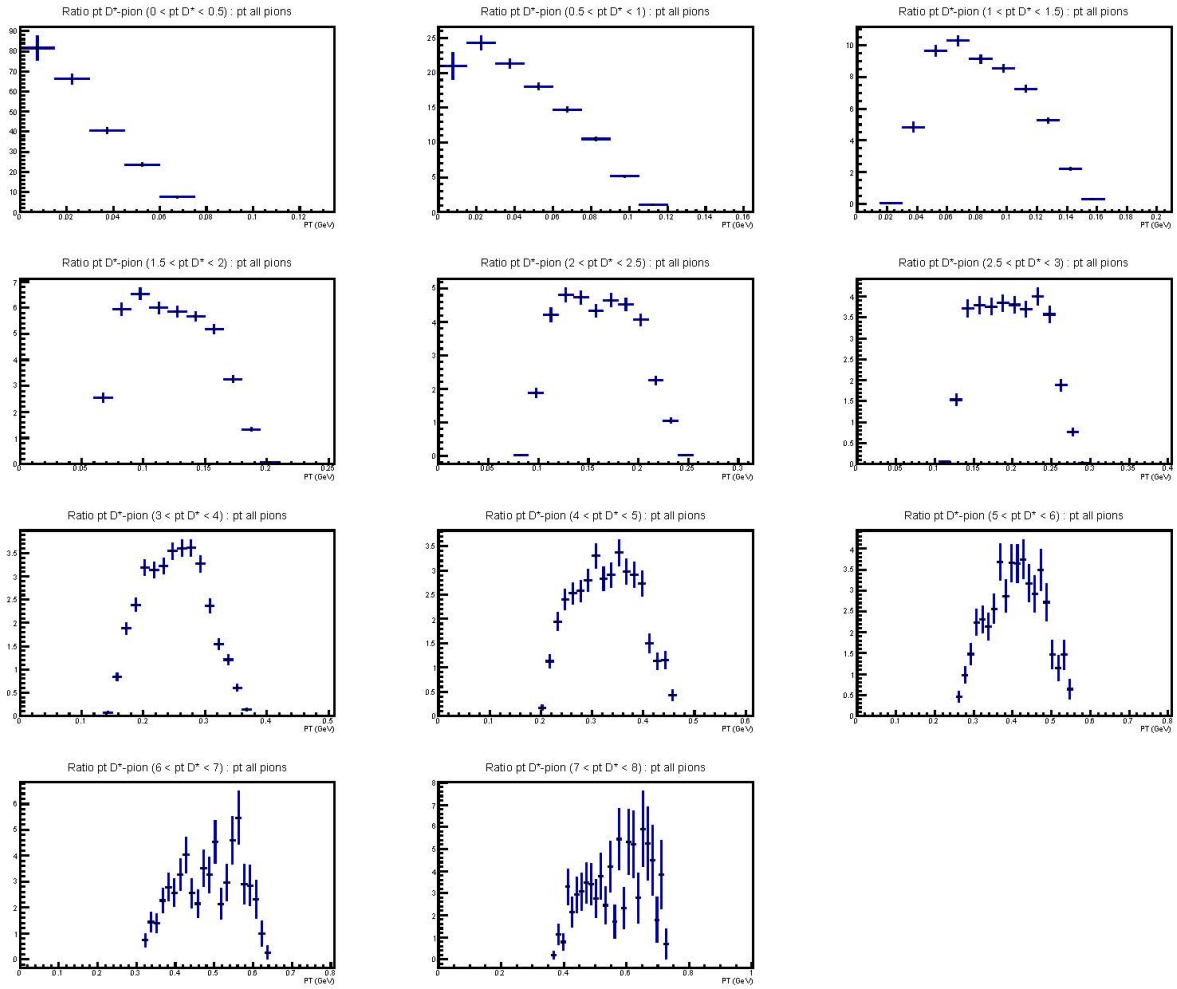

Figure 13: This figure shows the ratio between the probability distributions of the soft pion and the inclusive pions. Note, these are chance distributions, and do not provide information about absolute values.

Figure 14 shows us the ratio between the D^0 pions and the inclusive pions. Generally, the peaks of these graphs are at higher momentum, compared to the peaks in the ratio of the soft pions to the inclusive pions. However, when the momentum of the mother particle exceeds 4 GeV/c the shape changes to a more flat (soft) shape, and we can no longer speak about a peak, but instead about a maximum.

In figure 15 the simulated data is compared to the real data with the cuts determined in this thesis, see table 3, applied. However, as can be seen, this figure only shows 8 plots rather than 11. Up until the D^* particle having a momentum of 1 GeV/c, the data did not show any pions. Due to this, those plots have been left out. From the p_t range $1-1.5$ GeV/c there was very limited statistical information, hence, the p_t-bins $1-1.5$ GeV/c and $1.5-2$ GeV/c were merged together in order to still get information about low p_t-regions.

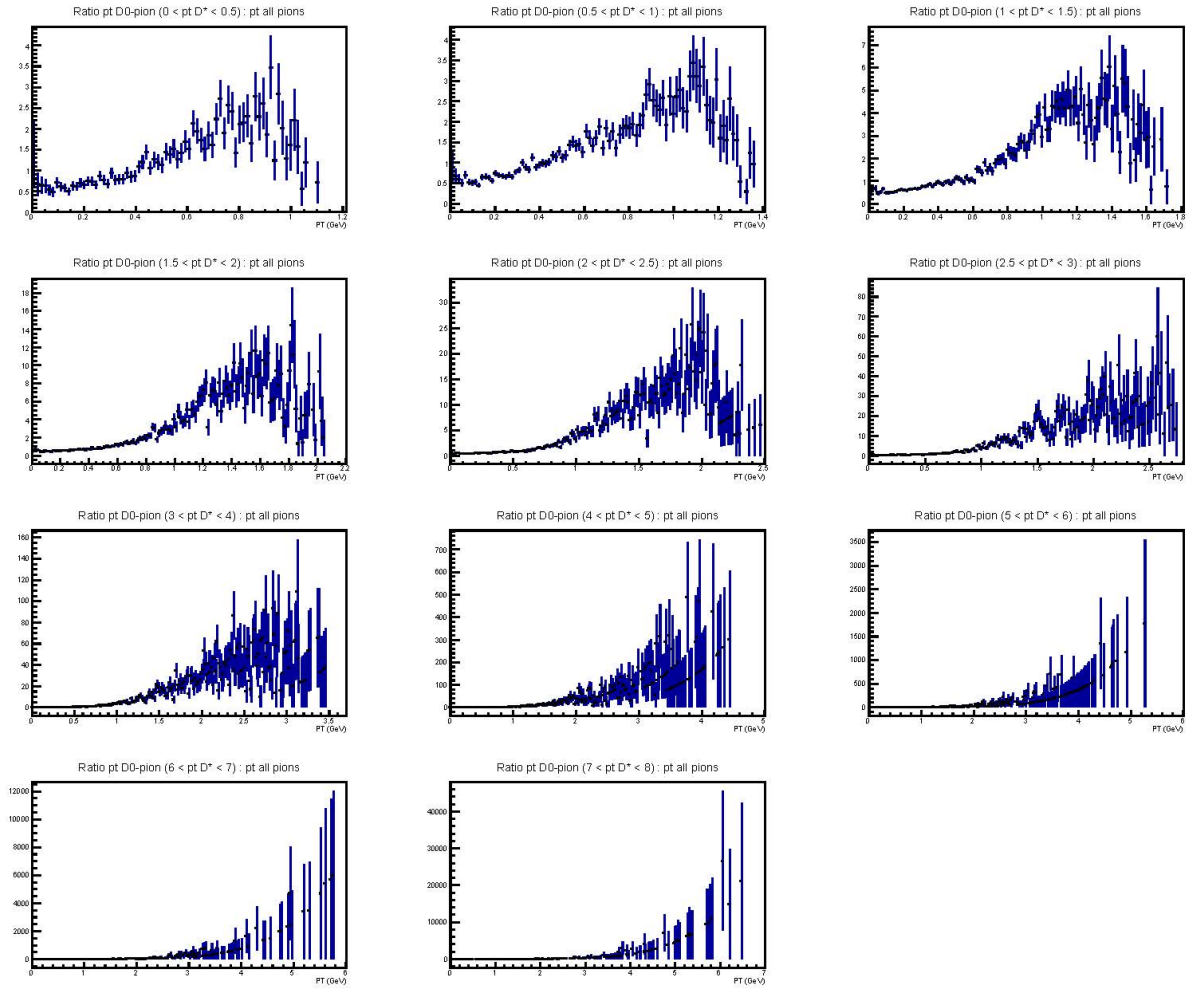

Figure 14: The ratio between the probability distributions of the D^0 pion and the inclusive pions are shown in this figure. Note, these are chance distributions, and do not provide information about absolute values.

For p_t values between 1 and 4 GeV/c, figure 15 shows that the simulated data and the measured data both have similar shapes, though the simulated data is in general a bit more broad then the measured data. From 4 GeV/c the shapes start to differ a bit. The measured data becomes a bit wider spread than the simulation, however, the peak of the pion signal remains at roughly the same p_t as the simulated data.

Figure 16) shows the invariant mass of the D^* particle with the background noise. In red, the background is fitted, in blue, the background plus the signal are fitted. At higher p_t values ($p_t > 4$ GeV/c) a Gaussian peak can clearly be distinguished. This Gaussian peak is the invariant mass of the D^* particle. The peak decreases, as the p_t of the D^* particle decreases, but nonetheless, a peak can be seen in the p_t-bins $2.5-3$ GeV/c and $3-4$ GeV/c. In the p_t-region $1-2$ GeV/c a slight bulge can be distinguished in the fit. The p_t-region $2-2.5$ GeV/c does not show any sign of a peak of some sorts.

Figures 17 and 18 are displayed to put the statistics of figure 16 of each p_T-bin in comparison with each other. In figure 17 the p_T value of the peak of the signal is showed for the p_T bins for which there was a clear signal. All peak values lie within 0.0006 GeV/c^2 from eachother. The world D^* mass value is 145.42 MeV/c [20], which agrees with our results. Figure 18 shows the width of the Gaussian signal. General research states that the σ of the D^* signal is 500 and 600 KeV/c^2, which is in agreement with the results found during this thesis. .

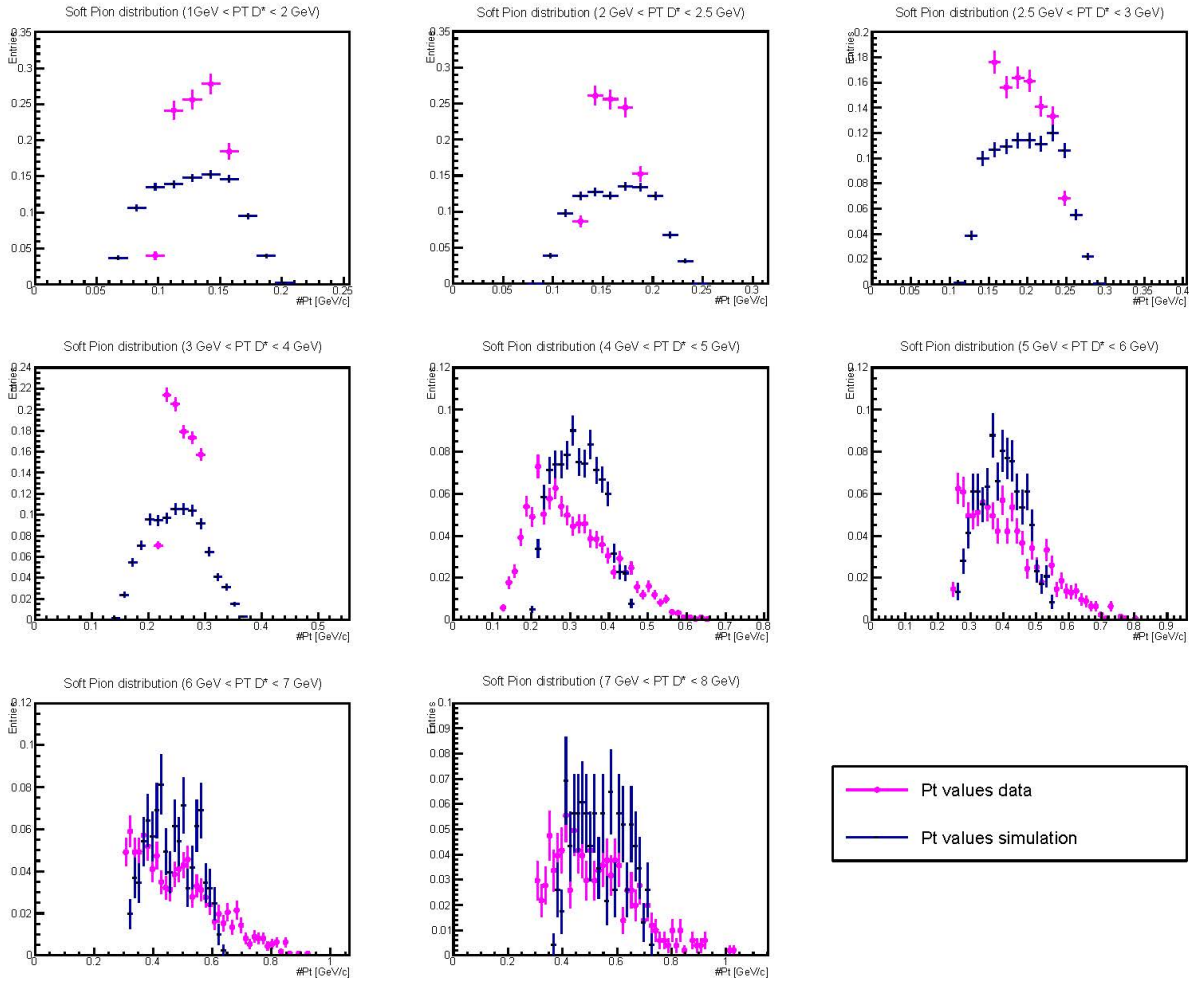

Figure 15: These plots show the comparison between the simulated soft pion p_T data, and the real data. The p_T of the soft pions in these plots range from 1-8 GeV/c.

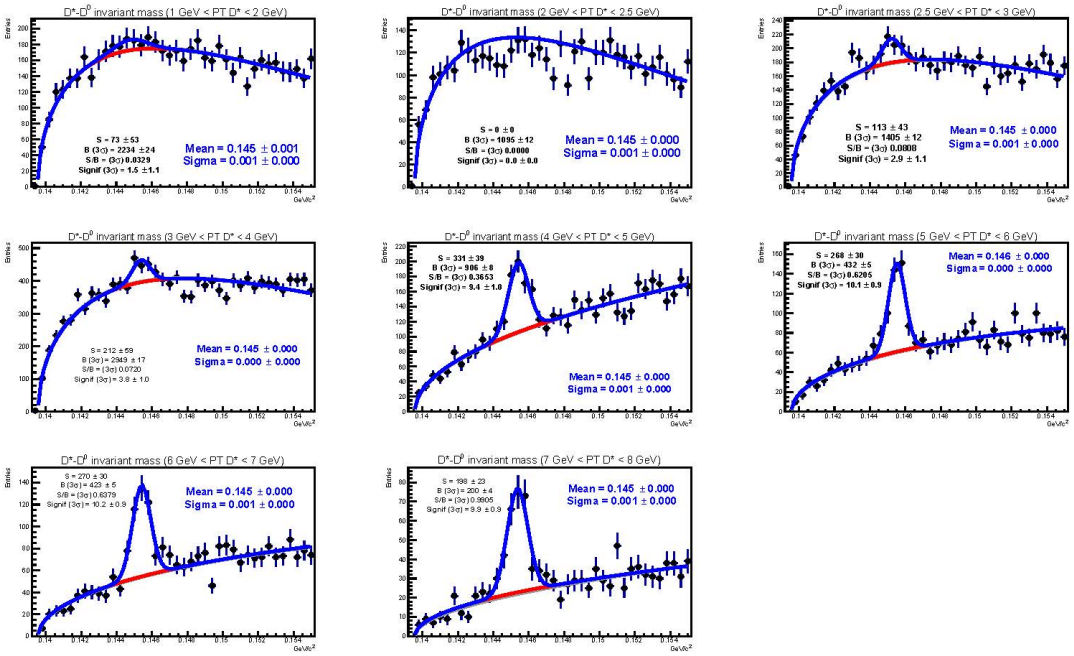

Figure 16: This figure shows the invariant mass plots of the D^* with the combinatorial background fitted. The p_T range of these plots is 1-8 GeV/c.

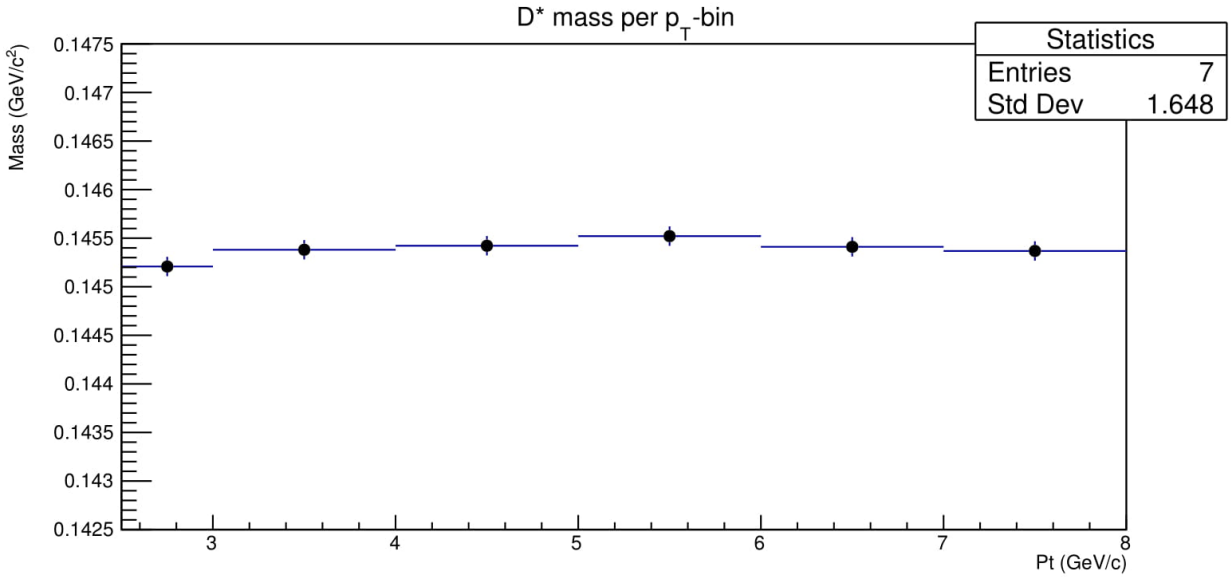

Figure 17: This figure shows the mass value of the peak of the signal from figure 16, for each p_T bin, ranging from 1-8 GeV/c.

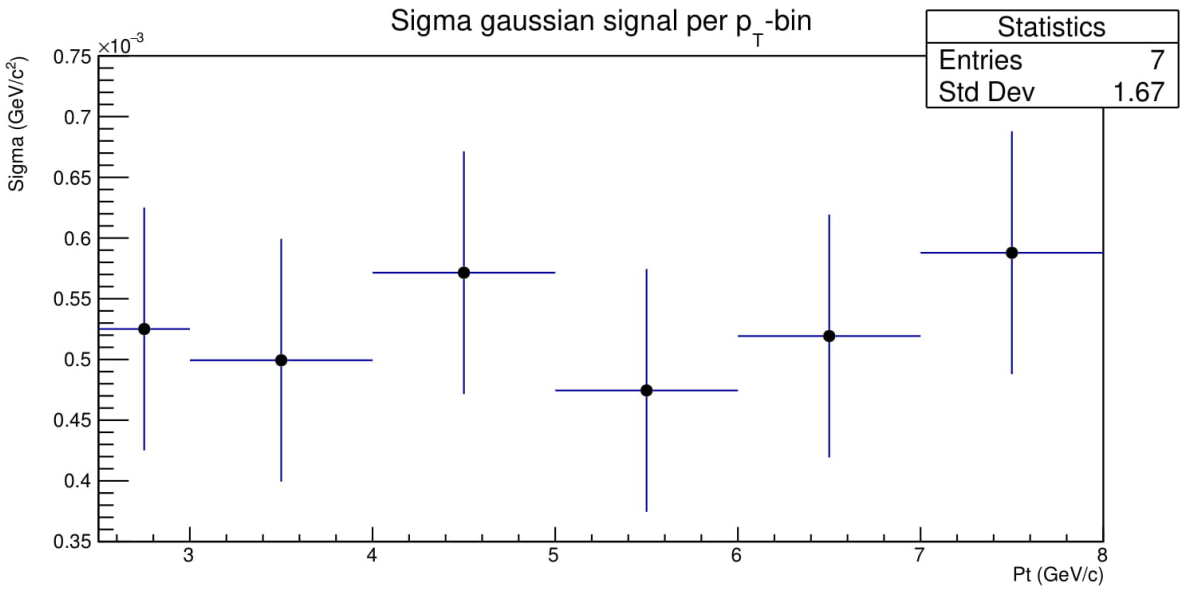

Figure 18: This figure shows the σ values from figure 16 for each p_T bin, ranging from 1-8 GeV/c.

6 Conclusion

From figures 9 and 12, we can conclude that at low p_T, it will be quite tough to seperate the D^0 pions from the background noise of all the pions created during the collision. This is because they have a large overlap in their p_t-regions both on a macro scale (all p_t values combined, figure 9) as well as on a micro scale (divided into p_t-bins, figure 12) as long as the p_t of the D^* does not exceed 5 GeV/c. The soft pion, however, is much more likely to be extracted from the background, due to its nature of having a very low p_t value compared to the mother particle, due to the mass of the D^0 particle created in that decay being close to the mass of the D^*, see figures 9 and 11. This allows us to use the soft pion p_T distribution to set effective kinematical cuts for the D^* reconstruction. Moreover, the study of the soft pion p_T provides evidence that it will never be possible to detect D^* mesons with a $p_T < 1$ GeV/c due to current detector limitations (ALICE cannot efficiently track below a p_T pf 100 MeV/c).

Figure 11 combined with figure 13 provides information on the p_T distribution of the soft pion within each of the selected D^* p_T-bins. It enables the determination of p_t cuts based on the p_t of the soft pion. These cuts are mentioned and stated in table 3 in section 5. Likewise, figures 12 and 14 show that the p_t of the D^0 pion in general is higher than the average pion created by the collision. However, for a D^* p_t larger than 4, the distribution shape becomes flatter.

From figure 15 we can conclude that the cuts that were made improved the data, meaning a lot of background noise was filtered, while the signal remained mostly untouched. At higher p_t values of the D^*, more background noise comes into play, so more cuts will have to be made for higher p_t values. For lower p_t values, the data resembled the simulation very well, meaning that more cuts based on the p_t of soft pions will not improve the signal by much, but rather will cut away a lot of signal and therefore a lot of statistics.

Finally, figure 16 shows that it is possible to go into p_t regions of the D^* lower than 3 GeV/c. Down to a p_t of 2.5 GeV/c, the signal is significant, meaning it stands more than 3 sigma significance above the background. Within the region 2-2.5 GeV/c, no statements can be made about the D^* particle, since a signal could not be distinguished from the background noise. The lowest region (1-2 GeV/c) shows us a slight bulge. This either could be a fluctuation of the background, or it could be a signal, it is impossible to exclude either of those options, considering the significance is too low. It does show that there is potential to find a signal at that low p_t regions, meaning that in the future it most likely will be possible to look at these regions, using more more precise detectors with a larger p_t range.

7 Discussion

The simulation studies done in this manuscript clearly point out that with the current ALICE detector, it is impossible to attempt the reconstruction of the D^* meson below a p_T of 1 GeV/c. Such statement comes from the fact that the average p_T of soft pions coming from a D^* of $p_T < 1$ GeV/c, lies below the minimum p_T the ALICE detector can measure (60-100 MeV/c).

However, ALICE is undergoing a major upgrade in 2019-2020, that among other upgrades consists of the installation of a new ITS detector with improved performances. The new improved detector is expected to highly increase the track reconstruction, pushing the p_T limit down to a threshold of 50 MeV/c. The simulation studies performed in this thesis show that at that point, it will be feasible to reconstruct the D^* meson down to extremely low momentum ($p_T \sim 0$ GeV/c).

Concerning the present detector, our simulation study shows that the reconstruction of the D^* meson should be possible down to a p_T of 1 GeV/c. Therefore, the fact, that in the data sample analyzed, it was not possible to reconstruct a clear mass peak below a p_T of 2.5 GeV/c, must come from the low statistic data sample used. As a continuation of this research, the first step should be to analyze the full data sample of 900 million p-p collisions in order to asses the situation. Furthermore, additional improvement could arise from a dedicated optimization of the topological cuts.

References

[1] Phys.org: The universes primordial soup flowing at CERN,
https://sciencesprings.wordpress.com/2016/02/26/from-phys-org-the-universes-primordial-soup-flowing-at-cern/

[2] Cern: Heavy ions and Quark-Gluon Plasma,
https://home.cern/science/physics/heavy-ions-and-quark-gluon-plasma

[3] Compstar: The QCD phase diagram and the critical end point,
https://compstar.uni-frankfurt.de/outreach/short-articles/the-qcd-phase-diagram-and-the-critical-end-point/

[4] Cern: Large Hadron Collider,
https://home.cern/science/accelerators/large-hadron-collider

[5] Cern: Alice Detector,
https://home.cern/science/experiments/alice

[6] Wikipedia: Alice Experiment,
https://en.wikipedia.org/wiki/ALICE_experiment

[7] Cern: More detail on the ALICE ITS,
http://alice.web.cern.ch/detectors/more-details-alice-its

[8] Cern: Present Inner Tracking System - Steps forward!,
http://alicematters.web.cern.ch/?q=ALICE_currentITS

[9] Cern: The ALICE Time Projection Chamber (TPC),
http://aliceinfo.cern.ch/Public/en/Chapter2/Chap2_TPC.html

[10] Nilsen, Bjorn S.: Heavy-flavor production in LHC pp interactions using the ALICE detector,
https://cds.cern.ch/record/1490903/plots

[11] Science direct: Particle identification of the ALICE TPC via dE/dx,
https://www.sciencedirect.com/science/article/pii/S0168900212005098

[12] Cern: More detail on the Time of Flight,
http://alice.web.cern.ch/detectors/more-details-time-flight

[13] Hyperphysics: Quarks,
http://hyperphysics.phy-astr.gsu.edu/hbase/Particles/quark.html

[14] Fabio Maltoni: Michele Selvaggi and Jesse Thaler: Exposing the dead cone effect with jet substructure techniques,
https://core.ac.uk/download/pdf/78072225.pdf

[15] Wikipedia: Color charge,
https://en.wikipedia.org/wiki/Color_charge

[16] Quora: Discovery of Omega-Minus,
https://www.quora.com/Could-someone-show-a-picture-of-a-collision-in-a-particle-accelerator-and-explain-in-laymans-terms-what-the-analysis-of-the-collision-is-1

[17] Andrea Dainese: Charm production and in-medium QCD energy loss in nucleusnucleus collisions with ALICE. A performance study.,
https://arxiv.org/pdf/nucl-ex/0311004.pdf

[18] Lund Monte Carlo,
http://home.thep.lu.se/~torbjorn/pythia81html/Welcome.html

[19] Cern: Root — A data analysis framework,
https://root.cern.ch/

[20] Particle Data Group: M. Tanabashi et al. (Particle Data Group), Phys. Rev. D 98, 030001 (2018),
http://pdg.lbl.gov/